The following Communications have been judged by at least two referees to be "very important papers" and will be published online at www.angewandte.org soon:

*T. J. Hebden, A. J. S. John, D. G. Gusev, W. Kaminsky, K. I. Goldberg, D. M. Heinekey**
Preparation of a Dihydrogen Complex of Cobalt

*T. Reiner, E. J. Keliher, S. Earley, B. Marinelli, R. Weissleder**
Synthesis and In Vivo Imaging of an ^{18}F-Labeled PARP1 Inhibitor by a Chemically Orthogonal Scavenger-Assisted High-Performance Method

Z. Zhao, E. L. Jacovetty, Y. Liu, H. Yan**
Encapsulation of Gold Nanoparticles in a DNA-Origami Cage

M. Barsukova-Stuckart, N. V. Izarova, G. B. Jameson, V. Ramachandran, Z. Wang, J. v. Tol, N. S. Dalal, R. N. Biboum, B. Keita, L. Nadjo, U. Kortz**
The Dicopper(II)-Containing 22-Palladate(II) $[Cu^{II}_2Pd^{II}_{22}P^{V}_{12}O_{60}(OH)_8]^{20-}$

F. Liao, Y. Huang, J. Ge, W. Zheng, K. Tedsree, P. Collier, X. Hong, S. C. Tsang**
Morphology-Dependent Interactions of ZnO with Cu Nanoparticles at the Materials Interface in the Selective Hydrogenation of CO_2 to CH_3OH

R. Langer, G. Leitus, Y. Ben-David, D. Milstein
Efficient Hydrogenation of Ketones Catalyzed by an Iron Pincer Complex

J. Vogelsang, J. Brazard, T. Adachi, J. C. Bolinger, P. F. Barbara*
Watching the Annealing Process One Polymer Chain at a Time

*H. Ishikawa, M. Honma, Y. Hayashi**
One-Pot Synthesis of a DPP4 Inhibitor by a Four-Component Coupling Reaction Mediated by Diphenylprolinol Silyl Ether

Author Profile

"If I could be anyone for a day, I would be Leonardo da Vinci.
My greatest achievement has been the design of a molecular motor. …"
This and more about Ben L. Feringa can be found on page 1470.

Books

Highlights

Hydrogen Production

One layer is enough: A new catalyst comprising a platinum monolayer on tungsten monocarbide (WC) could lead to inexpensive and efficient (photo)electrochemical production of molecular hydrogen (see scheme). The system uses far less platinum than conventional platinum-foil electrodes but is just as effective.

Minireviews

Reductive Elimination

K. M. Engle, T.-S. Mei, X. Wang,
J.-Q. Yu* ________ **1478 – 1491**

Bystanding F+ Oxidants Enable Selective Reductive Elimination from High-Valent Metal Centers in Catalysis

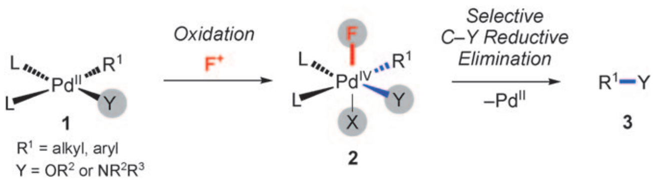

An emerging strategy for controlling the selectivity in reductive elimination from high-valent metal species is examined: using bystanding F$^+$ oxidants. Recent applications of this concept in Pd^{II}/Pd^{IV} and Au^{I}/Au^{III} catalysis are presented, along with a rare example in which one-electron oxidants have been used to promote selective reductive elimination in C–H functionalization.

Reviews

Materials Science

J. Ge, Y. Yin* ________ **1492 – 1522**

Responsive Photonic Crystals

Always good for an answer: Responsive photonic crystals fabricated by self-assembly processes can display photonic properties that can be tuned in response to external stimuli. These smart materials have wide applications in areas such as color displays, rewritable paper, optical switches, chemical and biological sensors, and antifraud devices.

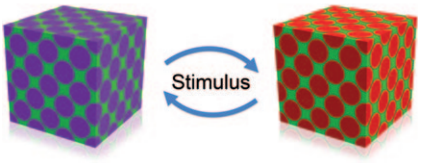

Synthetic Methods

A. Duschek, S. F. Kirsch* __ **1524 – 1552**

2-Iodoxybenzoic Acid—A Simple Oxidant with a Dazzling Array of Potential Applications

Oxidation made easy! 2-Iodoxybenzoic acid (IBX) has emerged as a universally applicable oxidizing agent. Besides the simple oxidation of alcohols, it is also suitable for dehydrogenations, oxygenations, and other oxidative processes (see picture), and has also found numerous applications in total synthesis.

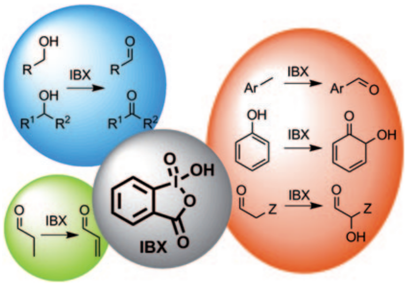

For the USA and Canada: ANGEWANDTE CHEMIE International Edition (ISSN 1433-7851) is published weekly by Wiley-VCH, PO Box 191161, 69451 Weinheim, Germany. Air freight and mailing in the USA by Publications Expediting Inc., 200 Meacham Ave., Elmont, NY 11003. Periodicals postage paid at Jamaica, NY 11431. US POSTMASTER: send address changes to *Angewandte Chemie*, Journal Customer Services, John Wiley & Sons Inc., 350 Main St., Malden, MA 02148-5020. Annual subscription price for institutions: US$ 9442/8583 (valid for print and electronic / print or electronic delivery); for individuals who are personal members of a national chemical society prices are available on request. Postage and handling charges included. All prices are subject to local VAT/sales tax.

Coordination Chemistry

R. Gramage-Doria, D. Armspach,*
D. Matt,* L. Toupet ——— **1554 – 1559**

A Cavity-Shaped Diphosphane Displaying "Oschelating" Behavior

A molecular balance wheel: Transition metals form β-cyclodextrin-derived diphosphane chelate complexes (picture: ligand structure) in which a fast oscillatory motion about the metal ion takes place ("oschelating behavior"). The observed movement occurs without dissociation of the metal–phosphorus bond.

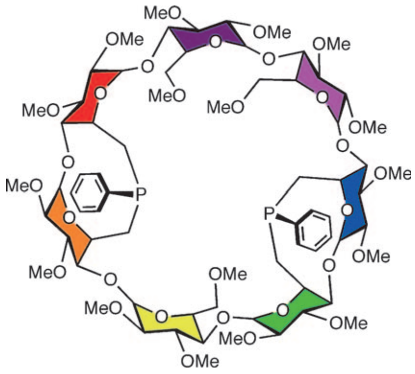

Metalloporphyrins

N. Motreff, S. Le Gac, M. Luhmer, E. Furet, J.-F. Halet, T. Roisnel,
B. Boitrel* ——— **1560 – 1564**

Formation of a Dinuclear Mercury(II) Complex with a Regular Bis-Strapped Porphyrin Following a Tunable Cooperative Process

Teamwork: Structural characterization of the first dinuclear mercury(II) complex with a regular porphyrin reveals dissymmetry induced by binding of dimethyl sulfoxide molecules to the metal ions, which form two allosterically connected binding sites (see structure; gray C, orange Hg, blue N, red O, yellow S). The cooperativity of the metal insertion can be tuned, either positively or negatively, by the presence of a base or by the interaction with exogenous ligands.

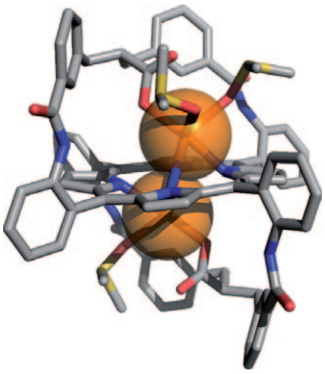

Photochromic Switches

S. Fukumoto, T. Nakashima,
T. Kawai* ——— **1565 – 1568**

Photon-Quantitative Reaction of a Dithiazolylarylene in Solution

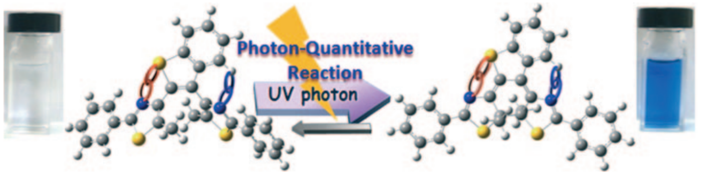

Ready for action: An excellent quantum yield was observed for a photocoloration reaction of a photochromic molecule based on a triangular terarylene structure. The molecule is brought into a conformation favorable for photocyclization by multiple intramolecular interactions, including CH—N hydrogen bonding and S—N and CH—π interactions (see picture).

Protein Nanoprobes

X. Lin, J. Xie, L. Zhu, S. Lee,* G. Niu, Y. Ma,
K. Kim, X. Chen* ——— **1569 – 1572**

Hybrid Ferritin Nanoparticles as Activatable Probes for Tumor Imaging

Rattling the cage: Protein cages are used as a scaffold to build protease-activatable probes. The self-assembly of ferritin cages generates hybrid proteins with matrix metalloproteinase (MMP)-specific activation (see picture). The formula with the highest activation efficiency is validated as a tumor-specific probe in a xenograft mouse model.

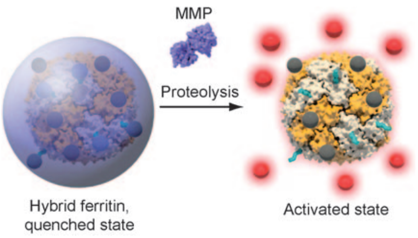

Magnetic Properties

J. L. Manson,* M. L. Warter,
J. A. Schlueter, T. Lancaster, A. J. Steele,
S. J. Blundell, F. L. Pratt, J. Singleton,
R. D. McDonald, C. Lee, M.-H. Whangbo,
A. Plonczak **1573 – 1576**

$[Cu(HF_2)_2(pyrazine)]_n$: A Rectangular Antiferromagnetic Lattice with a Spin Exchange Path Made Up of Two Different FHF^- Bridges

The two-dimensional antiferromagnet $[Cu(HF_2)_2(pyz)]_n$ (pyz = pyrazine) has a rectangular lattice (see picture) displaying two types of FHF^- bridging modes. The spin exchange through Cu-$(FHF)_2$-Cu is about 90% stronger than through Cu-pyz-Cu, and the $\mu_{1,1}$-coordinated FHF^-, which is close in nature to $F^-\cdots HF$, is largely responsible for the exchange. C black, Cu red, F green, H cyan.

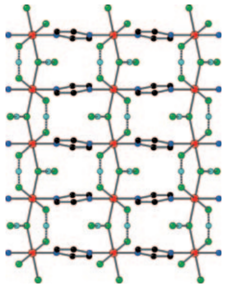

Hydrogels

C. M. Micklitsch, P. J. Knerr, M. C. Branco,
R. Nagarkar, D. J. Pochan,
J. P. Schneider* **1577 – 1579**

Zinc-Triggered Hydrogelation of a Self-Assembling β-Hairpin Peptide

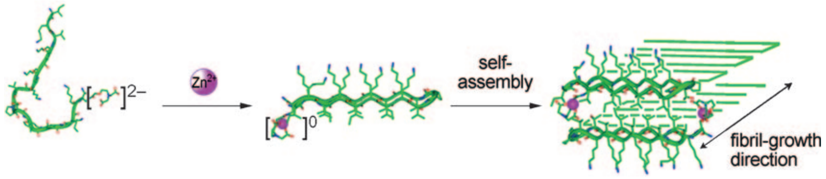

Zinc-chronized gelling: Selective zinc-triggered hydrogel formation is realized by the self-assembly of a de novo designed peptide (see picture). A non-natural, zinc-binding aminocarboxylate residue is incorporated into the peptide and is used to trigger folding, assembly, and subsequent gelation.

Asymmetric Synthesis

G. Dickmeiss, K. L. Jensen, D. Worgull,
P. T. Franke,
K. A. Jørgensen* **1580 – 1583**

An Asymmetric Organocatalytic One-Pot Strategy to Octahydroacridines

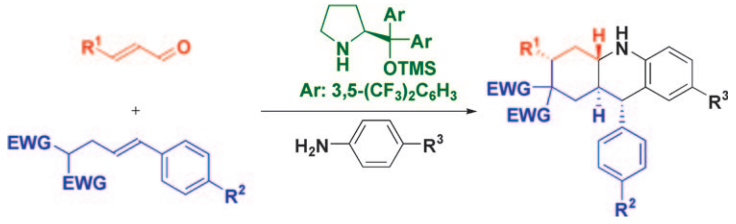

An elegant sequence: An efficient method for the formation of octahydroacridines provides high yields and a high level of stereogenic control, and displays great tolerance towards different aldehydes, anilines, and nucleophiles (see scheme; TMS = trimethylsilyl; EWG = electron-withdrawing group). The use of different nucleophiles verifies an *endo* transition state in which π–π overlap of the aromatic rings plays an important role in the reactivity and selectivity.

Heterogeneous Catalysis

E. de Smit, M. M. van Schooneveld,
F. Cinquini, H. Bluhm, P. Sautet,
F. M. F. de Groot,*
B. M. Weckhuysen* **1584 – 1588**

On the Surface Chemistry of Iron Oxides in Reactive Gas Atmospheres

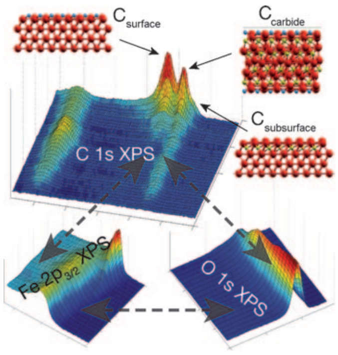

How details come to surface: The surface chemistry of small and large iron oxide crystallites was investigated in CO and H_2 by in situ XPS. Small particles reacted more dynamically to the changing experimental conditions than larger ones. Ab initio atomistic thermodynamics helped shed light on the enigmatic iron/carbon chemistry.

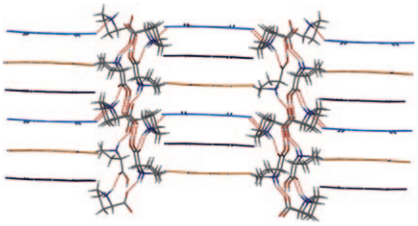

An attractive couple: $(\mathrm{Pro_2H^+})_2(\mathrm{TCNQ^{\bullet-}})_2\cdot\mathrm{TCNQ}$ (TCNQ = tetracyanoquinodimethane) contains an H-bonding network that supports a layered structure, composed of alternating TCNQ anions and proline cations (see picture). The cation is formed by two zwitterionic proline amino acids supported by a proton bridge between the carboxylates, whereas the anionic component involves a neutral TCNQ molecule sandwiched between two $\mathrm{TCNQ^{\bullet-}}$.

Amino Acid Semiconductor

X. Qu, J. Lu, C. Zhao, J. F. Boas, B. Moubaraki, K. S. Murray, A. Siriwardana, A. M. Bond,* L. L. Martin* ———— **1589 – 1592**

$(\mathrm{Pro_2H^+})_2(\mathrm{TCNQ^{\bullet-}})_2\cdot\mathrm{TCNQ}$: An Amino Acid Derived Semiconductor

---

Keeping in shape: The shapes of gold nanocrystals determine their self-assembly behavior—rhombic dodecahedral nanocrystals form triangular multilayers (see picture), whereas cubic and octahedral nanocrystals form monolayers or multilayers without well-defined contours. The three superstructures exhibit different optical properties, and the rhombic dodecahedral gold nanocrystals display strong anisotropic SERS effects.

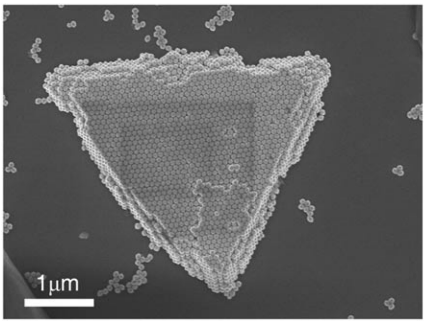

Nanostructures

Z. Zhu, H. Meng, W. Liu, X. Liu, J. Gong, X. Qiu, L. Jiang, D. Wang,* Z. Tang* ———— **1593 – 1596**

Superstructures and SERS Properties of Gold Nanocrystals with Different Shapes

---

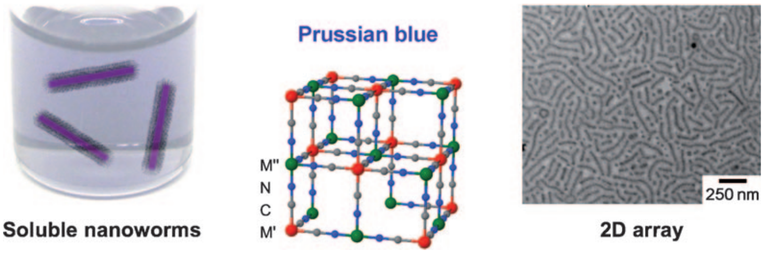

The nanoworm that turned: The self-assembly of a novel charged metal-containing diblock copolymer gives soluble nanoworms, which pack into two-dimensional arrays to form nanopatterned surfaces (see picture; M′,M″ = Fe, Zn, Cu, Co). The propensity of nanostructured metal–organic frameworks to form bulk crystals is thus overcome.

Metal–Organic Frameworks

X. Roy, J. K.-H. Hui, M. Rabnawaz, G. Liu, M. J. MacLachlan* ———— **1597 – 1602**

Soluble Prussian Blue Nanoworms from the Assembly of Metal–Organic Block Ionomers

---

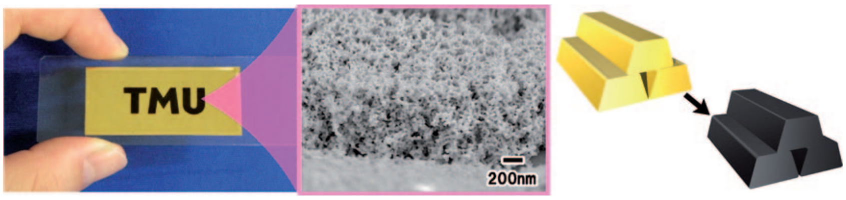

Black gold, but no oil: A nanoporous black gold film was formed by the anodization of gold in oxalate solution. The film had a spongelike porous configuration with a uniform hole size of approximately 20 nm (see picture). The formation mechanism has not yet been clarified, but carbonaceous matter produced by the anodic reaction of oxalate ions likely contributes to the growth of numerous nanopores on the gold anode.

Nanoporous Materials

K. Nishio,* H. Masuda ———— **1603 – 1607**

Anodization of Gold in Oxalate Solution To Form a Nanoporous Black Film

Bioconjugates

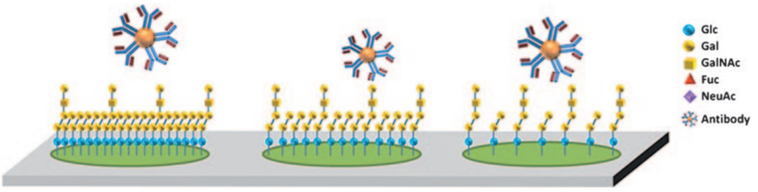

Who can? Glycan! Heterogeneous glycan microarrays were prepared for the study of antibody binding specificity and affinity. It was found that heterogeneous glycans provide better binding affinity compared to their individual components (see picture), thereby suggesting a new strategy for carbohydrate-based vaccine design.

Organocatalysis

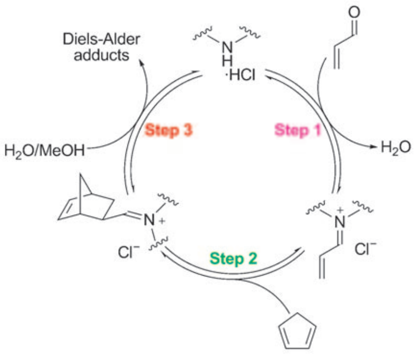

Step by step: The effect of protic solvents on the rate and stereochemical outcome of the imidazolidinone-catalyzed Diels–Alder cycloaddition was rationalized. The following picture emerges: the solvent accelerates iminium ion formation (step 1), the Diels–Alder cycloaddition is reversible (step 2), and the solvent intercepts the iminium ion adduct (step 3).

Nanoparticle Assembly

Deposition under control: Silica nanoparticles with finely controllable size and surface charge were synthesized under benign conditions. By adjusting the electrostatic interactions, the silica nanoparticles can be assembled onto inorganic and biological surfaces in a controllable fashion. Potential uses for cell encapsulation are demonstrated.

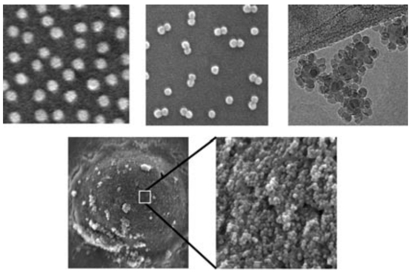

Self-Seeding Micelles

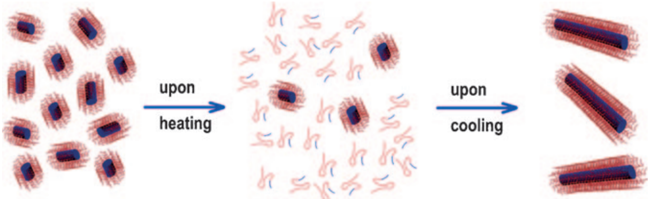

Do it yourself: When short fragments (ca. 50 nm) of rodlike PI-PFS block copolymer micelles in decane are heated above a characteristic temperature (60 °C) and then cooled to room temperature, a smaller number of longer micelles with a narrow length distribution are obtained. This process resembles self-seeding of polymer crystals, involving selective dissolution of the fragments of the lowest degree of crystallinity with the surviving submicroscopic seeds acting as nuclei for the growth of micelles upon cooling.

Photochemistry

S. Ji, W. Wu, W. Wu, H. Guo,
J. Zhao* 1626–1629

Ruthenium(II) Polyimine Complexes with a Long-Lived ^{3}IL Excited State or a ^{3}MLCT/^{3}IL Equilibrium: Efficient Triplet Sensitizers for Low-Power Upconversion

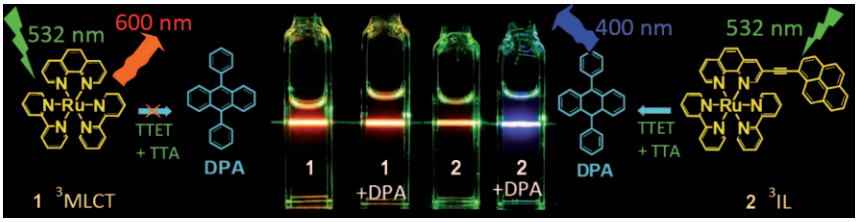

Up, up, and away! The long-lived ^{3}IL excited states of Ru^{II} polyimine complexes were found to be more efficient in sensitizing upconversion based on triplet–triplet annihilation (TTA) and energy transfer (TTET) than the shorter-lived ^{3}MLCT excited states (see picture). Upconversion occurs with an anti-Stokes shift of up to 0.77 eV.

Polyketides

L. Ding, A. Maier, H.-H. Fiebig, H. Görls, W.-H. Lin, G. Peschel,
C. Hertweck* 1630–1634

Divergolides A–D from a Mangrove Endophyte Reveal an Unparalleled Plasticity in ansa-Macrolide Biosynthesis

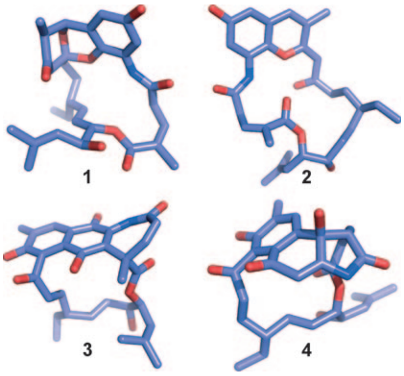

In-built diversification: Four ansa macrolides, divergolides A–D (**1**–**4**), with intriguing structures were isolated from a bacterial endophyte of the mangrove tree *Bruguiera gymnorrhiza*. These compounds are generated by a common biogenesis from a linear precursor that undergoes various reactions to give the multicyclic structures. This remarkable plasticity results in metabolites with different antibacterial and cytotoxic properties.

Glycopeptide Vaccines

B. L. Wilkinson, S. Day, L. R. Malins, V. Apostolopoulos,
R. J. Payne* 1635–1639

Self-Adjuvanting Multicomponent Cancer Vaccine Candidates Combining Per-Glycosylated MUC1 Glycopeptides and the Toll-like Receptor 2 Agonist Pam$_3$CysSer

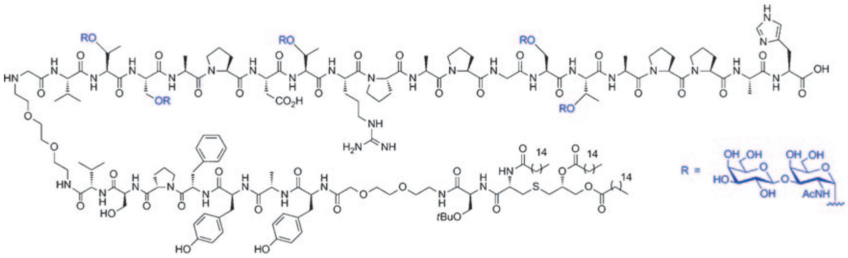

More sugar with your "T": The title candidates comprising per-glycosylated MUC1 peptides, a T-cell helper peptide, and an immunoadjuvant were assembled in high yields using iterative pentafluorophenyl ester-mediated fragment condensations. Following immunological evaluation, a tricomponent vaccine bearing clustered glycosylation with the T-antigen was identified (see structure) which elicited high IgG antibody titers in murine models without an external adjuvant.

Foldamers

Z. Yu, S. Hecht* 1640–1643

Reversible and Quantitative Denaturation of Amphiphilic Oligo(azobenzene) Foldamers

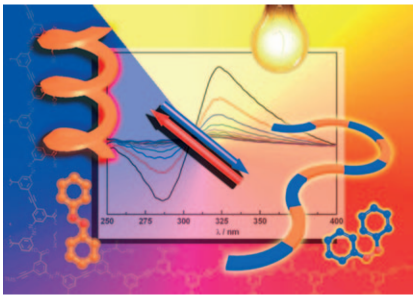

Light-driven spring: Smart photoswitchable foldamers composed entirely of azobenzene repeat units adopt stable helical structures in the dark and can be readily and reversibly unfolded upon UV irradiation as indicated by vanishing circular dichroism signals (see picture). Variation of the oligomer length leads to optimization of the performance of the foldamers and hence quantitative light-induced unfolding and re-folding.

Imaging Agents

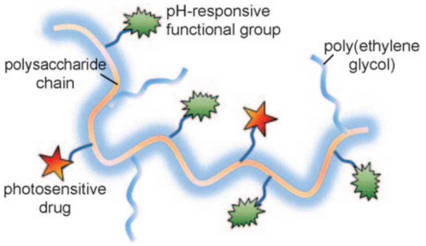

Sharper image: A newly developed polysaccharide/drug conjugate (see picture) responds to changes in pH value and was shown to penetrate HeLa tumors in mice as determined by fluorescence imaging. It has the potential to be used in photodynamic therapy, thereby targeting the tumor while having no detrimental effects on the surrounding tissue.

Polymer Vesicles

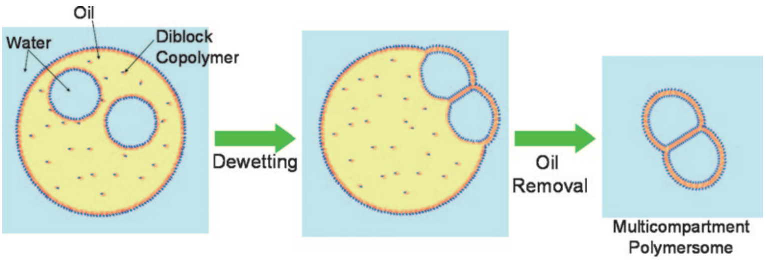

Versatile chambers: A microfluidic technique is used to generate polymersomes with multiple compartments using double emulsions with different morphology as templates (see scheme). The polymersomes could be utilized for encapsulation of multiple substances and as reaction vessels that enable triggered reaction with controlled stoichometry of the reactants.

Radical Ligands

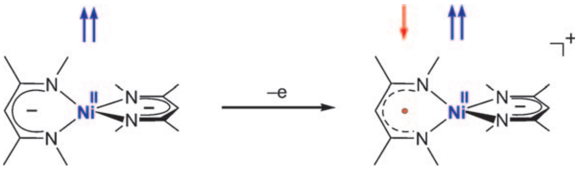

End of innocence: A β-diketiminate(1−) ligand, formerly thought to be innocent, is shown to be redox-active: It can undergo one-electron oxidation to form a neutral π radical stabilized by coordination to a high-spin Ni^{II} ion (see scheme). However, since the change in oxidation state of the ligand does not significantly change intraligand bond lengths, its noninnocence is hidden from X-ray crystallography.

Synthetic Ion Channels

Pretty choosy: The selectivity filters of biological ion channels serve as inspiration for the development of ionophore-modified solid-state nanopores exhibiting extraordinary ion selectivity (see picture). Potentiometric transduction is introduced as a simple means to demonstrate the ion-sensing capability of such nanopores.

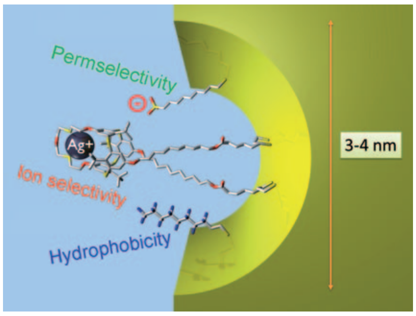

Self-Healing Materials

Y. Amamoto, J. Kamada, H. Otsuka,
A. Takahara,
K. Matyjaszewski* ———— 1660 – 1663

Repeatable Photoinduced Self-Healing of Covalently Cross-Linked Polymers through Reshuffling of Trithiocarbonate Units

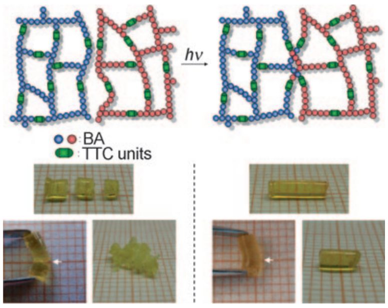

Well-healed: Polymers cross-linked with trithiocarbonate (TTC) units were prepared by a RAFT polymerization. The repeatable self-healing systems or macroscopic fusions were accomplished by UV irradiation of the cross-linked polymer in solution and in the bulk state. The macroscopic fusion of completely separated parts was successful (see pictures, BA = *n*-butyl acrylate).

Asymmetric Catalysis

M. Kobayashi, T. Suda, K. Noguchi,
K. Tanaka* ———— 1664 – 1667

Enantioselective Construction of Bridged Multicyclic Skeletons: Intermolecular [2+2+2] Cycloaddition/Intramolecular Diels–Alder Reaction Cascade

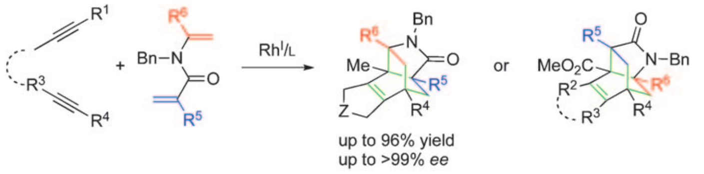

Bridging a gap: A cationic rhodium(I)/ligand complex catalyzes the title reaction of alkynes and amide-linked 1,5-dienes, leading to bridged multicyclic compounds, with high chemo-, regio-, and enantioselectivity (see scheme; Bn = benzyl).

Multinuclear Complexes

E. Y. Tsui, M. W. Day,
T. Agapie* ———— 1668 – 1672

Trinucleating Copper: Synthesis and Magnetostructural Characterization of Complexes Supported by a Hexapyridyl 1,3,5-Triarylbenzene Ligand

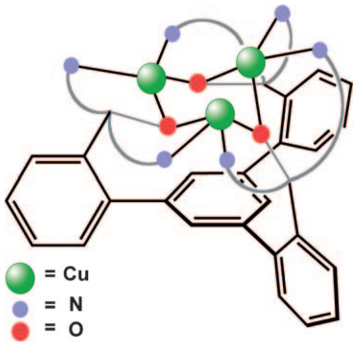

Copper threesome: A hexapyridyl ligand based upon a 1,3,5-triphenylbenzene framework coordinates three metal centers in a constrained environment (see picture). The tricopper(I) complex reduces dioxygen to form a tricopper(II) cluster. The capping anions affect the magnetism and EPR spectra of these species and reveal a linear dependence between the antiferromagnetic exchange parameter and the Cu-O-Cu angles.

N-Heterocyclic Carbenes

J. Mahatthananchai, P. Zheng,
J. W. Bode* ———— 1673 – 1677

α,β-Unsaturated Acyl Azoliums from N-Heterocyclic Carbene Catalyzed Reactions: Observation and Mechanistic Investigation

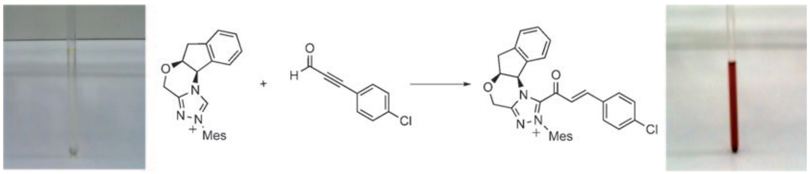

Caught in the act: Acyl azoliums have long been thought to be key reactive intermediates in N-heterocyclic carbene catalysis, but they have never been observed under catalytic conditions. Now, this has been successfully achieved by the characterization of α,β-unsaturated acyl azoliums (see scheme) using different spectroscopic techniques. Kinetic studies revealed the origin of their unexpected chemoselectivity in acylation and annulation reactions.

Asymmetric Catalysis

D. T. Cohen, B. Cardinal-David,
K. A. Scheidt* 1678 – 1682

Lewis Acid Activated Synthesis of Highly Substituted Cyclopentanes by the N-Heterocyclic Carbene Catalyzed Addition of Homoenolate Equivalents to Unsaturated Ketoesters

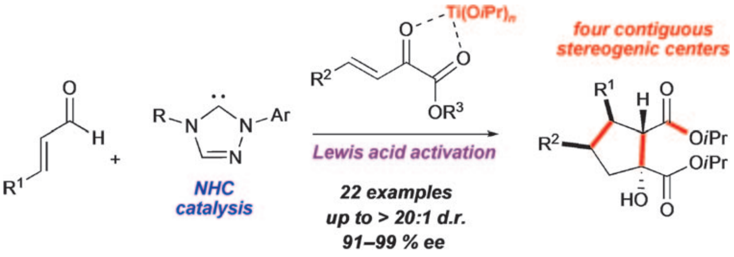

A great team: Cyclopentanes with four contiguous stereogenic centers were assembled with excellent diastereo- and enantioselectivity from simple β,γ-unsaturated α-ketoesters and enals in a reaction catalyzed by an N-heterocyclic carbene (NHC) and mediated by a titanium(IV) Lewis acid (see scheme). The presence of a Lewis acid was essential for the desired transformation to occur.

Fiber Supercapacitors

J. Bae, M. K. Song, Y. J. Park, J. M. Kim,*
M. Liu, Z. L. Wang* 1683 – 1687

Fiber Supercapacitors Made of Nanowire-Fiber Hybrid Structures for Wearable/Flexible Energy Storage

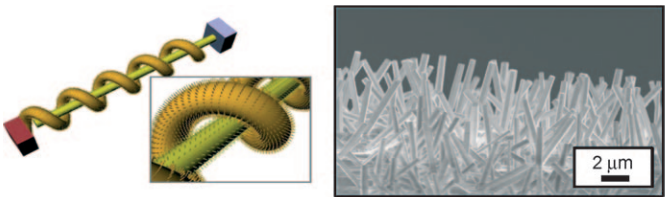

Current clothing trends: A wearable and flexible fiber supercapacitor with a fully encapsulated electrolyte is formed by wrapping a plastic wire covered with ZnO nanowires (NWs; see SEM image) around a Kevlar fiber covered with gold-coated ZnO NWs. This supercapacitor shows promise as a highly efficient, wearable energy storage device.

Synthetic Methods

A. J. Grenning, J. A. Tunge* 1688 – 1691

Deacylative Allylation of Nitroalkanes: Unsymmetric Bisallylation by a Three-Component Coupling

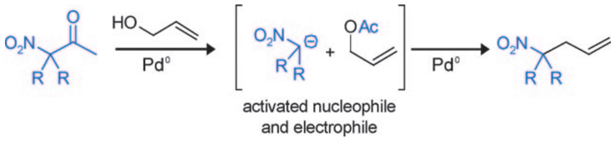

Use it and lose it! Allylic alcohols were used directly for the synthesis of diallylated nitroalkanes in a three-component coupling based on the strategy of deacylative allylation for the in situ generation of a nucleophile and an allyl electrophile (see scheme).

Homogeneous Catalysis

K.-H. Kwon, D. W. Lee,
C. S. Yi* 1692 – 1695

Tetrasubstituted Olefins through the Stereoselective Catalytic Intermolecular Conjugate Addition of Simple Alkenes to α,β-Unsaturated Carbonyl Compounds

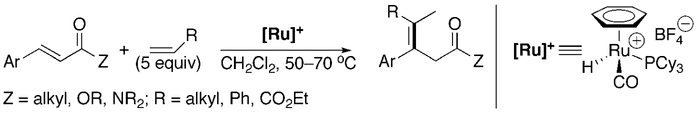

Branching out: The cationic ruthenium–hydride complex **[Ru]**$^+$ was found to be a highly effective catalyst precursor for the conjugate addition of unactivated olefins to α,β-unsaturated carbonyl compounds to yield tetrasubstituted olefins. A kinetic analysis provides support for the mechanism involving a regioselective olefin insertion and rapid alkene isomerization steps.

Selective memory: Using actinides in designing molecular nanomagnets could provide better performance and higher anisotropy barriers, owing to the peculiar properties of the 5f electron shell. Neptunocene is found to display an open magnetic hysteresis cycle at low temperatures (see picture), and interaction with the hyperfine degrees of freedom determines whether the magnetic relaxation is fast or slow at a given field value.

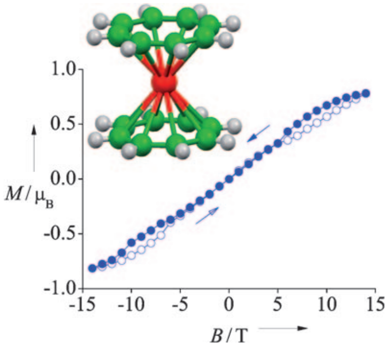

Actinide Magnetochemistry

N. Magnani, C. Apostolidis,
A. Morgenstern, E. Colineau, J.-C. Griveau,
H. Bolvin, O. Walter,
R. Caciuffo* ________ **1696 – 1698**

Magnetic Memory Effect in a Transuranic Mononuclear Complex

An active contribution: The specific capacitance of carbon-based supercapacitors can be significantly improved by the addition of an electrochemically active compound (hydroquinone) to the supporting electrolyte. The strong contribution of the redox-active electrolyte to the pseudocapacitance of the system results in the largest capacitance values obtained for an activated carbon-based supercapacitor.

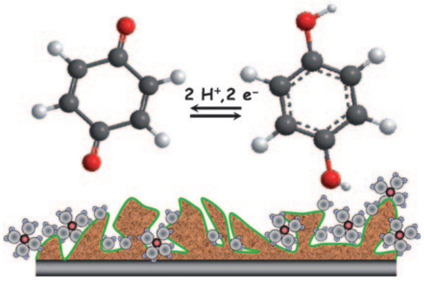

Energy Storage

S. Roldán, C. Blanco, M. Granda,
R. Menéndez,
R. Santamaría* ________ **1699 – 1701**

Towards a Further Generation of High-Energy Carbon-Based Capacitors by Using Redox-Active Electrolytes

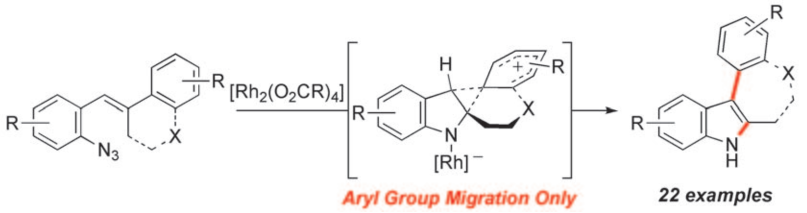

Rings à la carte: Rhodium carboxylate complexes catalyze selective cascade reactions to produce a range 2,3-disubstituted indoles from β,β-disubstituted stryryl azides. The selective migration of aryl groups appears to originate from a putative phenonium ion reactive intermediate (see scheme).

Heterocyclic Synthesis

K. Sun, S. Liu, P. M. Bec,
T. G. Driver* ________ **1702 – 1706**

Rhodium-Catalyzed Synthesis of 2,3-Disubstituted Indoles from β,β-Disubstituted Stryryl Azides

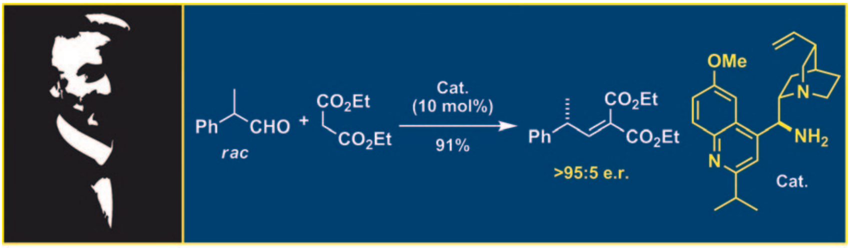

116 years after the discovery of the Knoevenagel condensation, the first catalytic asymmetric variant has been developed. Dynamic kinetic resolution in the reaction of α-branched aldehydes with malonates in the presence of a newly designed and readily available modified cinchona amine catalyst gives the corresponding alkylidene malonates in high enantioselectivity (see scheme).

Aminocatalysis

A. Lee, A. Michrowska, S. Sulzer-Mosse,
B. List* ________ **1707 – 1710**

The Catalytic Asymmetric Knoevenagel Condensation

Bioinorganic Chemistry

F. F. Pfaff, S. Kundu, M. Risch, S. Pandian, F. Heims, I. Pryjomska-Ray, P. Haack, R. Metzinger, E. Bill, H. Dau, P. Comba, K. Ray* ________ **1711 – 1715**

An Oxocobalt(IV) Complex Stabilized by Lewis Acid Interactions with Scandium(III) Ions

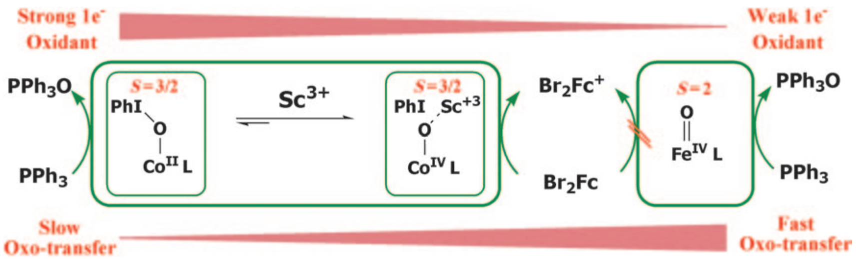

An elusive $S = 3/2$ oxocobalt(IV) complex is stabilized by a Lewis acid interaction with a scandium(III) ion. The $\{Co^{IV}\text{-}O\text{-}Sc\}^{3+}$ unit, characterized by spectroscopic and DFT methods, is a stronger electron-transfer and H-atom abstraction agent but weaker oxo-transfer agent than the corresponding $\{Fe^{IV}{=}O\}$ complex (see scheme; L = tris[2-(*N*-tetramethylguanidyl)ethyl]-amine).

Gas-Phase MgO Clusters

K. Kwapien, M. Sierka,* J. Döbler, J. Sauer, M. Haertelt, A. Fielicke,* G. Meijer ________ **1716 – 1719**

Structural Diversity and Flexibility of MgO Gas-Phase Clusters

Working out the gas charge: Only one structure type is known for bulk MgO. In contrast, quantum chemical calculations combined with infrared multiple photon dissociation experiments demonstrate that neutral and cationic gas-phase clusters of MgO display unusual structural diversity and flexibility (see picture).

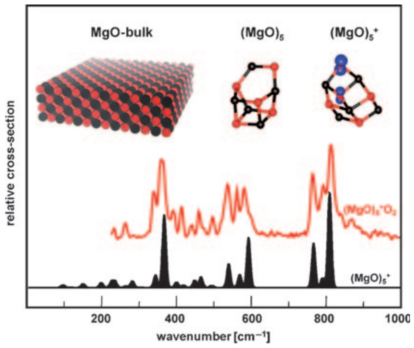

Diazirinone

X. Zeng, H. Beckers,* H. Willner,* J. F. Stanton ________ **1720 – 1723**

Elusive Diazirinone, N_2CO

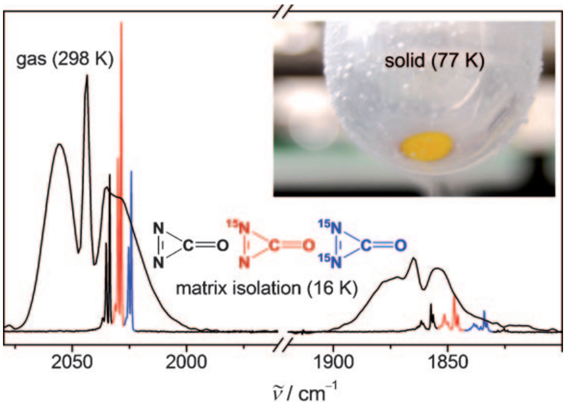

In a flash: Diazirinone, N_2CO, a mixed dimer of the two most strongly bonded diatomic molecules N_2 and CO, has been prepared by low-pressure pyrolysis of carbonyl diazide, $OC(N_3)_2$, and trapped at 77 K as a yellow solid. It was characterized by IR (gas-phase and matrix-isolation) spectroscopy, and its structure, which retains the N–N and C–O bonds, was unambiguously confirmed by the vibrational pattern of the two distinct ^{15}N isotopologues.

Supporting information is available on www.angewandte.org (see article for access details).

A video clip is available as Supporting Information on www.angewandte.org (see article for access details).

This article is available online free of charge (Open Access)

Service